Open access • Posted Content • DOI:10.1101/757575

Loss ofO-linked protein glycosylation inBurkholderia cenocepaciaimpairs biofilm formation and siderophore production via alteration of quorum sensing regulation

— **Source link** ↗

Cameron C. Oppy, Leila Jebeli, Miku Kuba, Clare V. Oates ...+11 more authors

Institutions: University of Melbourne, Monash University, New York University, University of Western Ontario ...+2 more institutions

Topics: Burkholderia cenocepacia, Glycosylation, Glycoprotein, Regulon and Virulence

Related papers:

- Loss of O -Linked Protein Glycosylation in Burkholderia cenocepacia Impairs Biofilm Formation and Siderophore Activity and Alters Transcriptional Regulators.

- DNA methylation epigenetically regulates gene expression in Burkholderia cenocepacia and controls biofilm formation, cell aggregation, and motility

- DNA methylation epigenetically regulates gene expression in Burkholderia cenocepacia

- A ten gene-containing genomic island determines flagellin glycosylation: implication for its regulatory role in motility and virulence of Xanthomonas oryzae pv. oryzae

- σ54-Dependent Response to Nitrogen Limitation and Virulence in Burkholderia cenocepacia Strain H111

Share this paper:

View more about this paper here: https://typeset.io/papers/loss-ofo-linked-protein-glycosylation-inburkholderia-r6yk2gp4yd

Loss of *O*-linked protein glycosylation in *Burkholderia cenocepacia* impairs biofilm formation and siderophore production via alteration of quorum sensing regulation

Cameron C. Oppy[1,2*], Leila Jebeli[1*], Miku Kuba[1], Clare V. Oates[1], Richard Strugnell[1], Laura E. Edgington-Mitchell[2-4], Miguel A. Valvano[5,6], Elizabeth L. Hartland[1,7,8], Hayley J. Newton[1], Nichollas E. Scott[1]

[1]Department of Microbiology and Immunology, University of Melbourne at the Peter Doherty Institute for Infection and Immunity, Melbourne 3000, Australia

[2]Bio21 Molecular Science and Biotechnology Institute, University of Melbourne, Victoria 3010, Australia

[3]Drug Discovery Biology, Monash Institute of Pharmaceutical Sciences, Monash University, Parkville, VIC, Australia

[4]Department of Oral and Maxillofacial Surgery, New York University College of Dentistry, Bluestone Center for Clinical Research, New York, New York, USA

[5]Wellcome-Wolfson Institute for Experimental Medicine, Queen's University Belfast, Belfast, BT97BL, United Kingdom

[6]Department of Microbiology and Immunology, University of Western Ontario, London, ON, N6A 5C1, Canada

[7]Centre for Innate Immunity and Infectious Diseases, Hudson Institute of Medical Research, Clayton, Victoria, Australia

[8]Department of Molecular and Translational Science, Monash University, Clayton, Victoria, Australia

*These authors contributed equally

Abstract

O-linked protein glycosylation is a conserved feature of the *Burkholderia* genus. For *Burkholderia cenocepacia*, the addition of the trisaccharide β-Gal-(1,3)-α-GalNAc-(1,3)-β-GalNAc to membrane exported proteins is required for virulence and resistance to environmental stress. However, the underlying causes of the defects observed in the absence of glycosylation are unclear. This study demonstrates that the global *B. cenocepacia* proteome undergoes dramatic changes consistent with alterations in global transcriptional regulation in the absence of glycosylation. Using luciferase reporter assays and DNA cross-linking analysis, we confirm the repression of the master quorum sensing regulon CepR/I in response to the loss of glycosylation, which leads to the abolition of biofilm formation, defects in siderophore production, and reduced virulence. The abundance of most of the known glycosylated proteins did not significantly change in the glycosylation-defective mutants except for BCAL1086 and BCAL2974, which were found in reduced amount, suggesting they could be degraded. However, the loss of these two proteins was not responsible for driving the proteomic alterations, as well as for reduced virulence and siderophore production. Together, our results show that loss of glycosylation in *B. cenocepacia* results in a global cell reprogramming via alteration of the CepR/I regulon, which cannot be explained by the abundance changes in known *B. cenocepacia* glycoproteins.

IMPORTANCE

Protein glycosylation is increasingly recognised as a common protein modification in bacterial species. Despite this commonality our understanding of the role of most glycosylation systems in bacterial physiology and pathogenesis is incomplete. In this work, we investigated the effect of the disruption of *O*-linked glycosylation in the opportunistic pathogen *Burkholderia cenocepacia* using a combination of proteomic, molecular and phenotypic assays. We find that in contrast to recent findings on the *N*-linked glycosylation systems of *Campylobacter jejuni,* *O*-linked glycosylation does not appear to play a role in proteome stabilization of most glycoproteins. Our results reveal that virulence attenuation observed within glycosylation-null *B. cenocepacia* strains are consistent with alteration of the master virulence regulator CepR. The repression of CepR transcription and its associated phenotypes support a model in which the virulence defects observed in glycosylation-null strains are at least in part due to transcriptional alteration and not the direct result of the loss of glycosylation *per-se*. This research unravels the pleotropic effects of *O*-linked glycosylation in *B. cenocepacia,* demonstrating that its loss does not simply affect the stability of the glycoproteome, but also interferes with transcription and the broader proteome.

Introduction

The *Burkholderia cepacia complex* (Bcc) includes diverse and ubiquitous, phylogenetically related Gram-negative species (1). To-date, 20 Bcc species have been identified (1-3), but the commonality of Bcc in the environment (2, 3) and their recognition as opportunistic pathogens (4-6) continually drives the identification of new Bcc members. Within clinical settings Bcc can lead to fatal infections (7, 8) which are both challenging to control with antibiotic therapies (9) and can be spread by patient-to-patient transmission (10, 11). This is especially problematic for Bcc infections within cystic fibrosis (CF) patients, where Bcc infections result in accelerated loss of lung function (12) as well as increased morbidity and mortality compared to other infectious agents (13, 14). *B. cenocepacia* is one of the most common Bcc species isolated from CF patients across the globe (15-18) and is generally associated with more fulminant disease leading to higher mortality than observed with other Bcc species (19). One of the most serious clinical outcomes from *B. cenocepacia* infections in CF patients is a condition known as 'cepacia syndrome', an unrelenting necrotizing pneumonia that rapidly leads to respiratory failure, bacteraemia and death (20). Although interventions with antimicrobial therapies can stop or even reverse cepacia syndrome (20), the intrinsic resistance of Bcc to multiple classes of antibiotic (21-23) and their propensity to form biofilms (24) makes treatment success variable at best (9). It is therefore essential to better understand factors involved in *B. cenocepacia* virulence in order to improve clinical outcomes.

The ability to form biofilms is associated with bacterial persistence and the failure of antimicrobial treatments in a range of pathogens (25). Bcc members, including *B. cenocepacia,* produce biofilms on abiotic (26, 27) and biotic surfaces (28). However, *B. cenocepacia* in the CF lung do not appear to form true biofilms, but instead are observed extracellularly as small clusters surrounded by mucus, or in phagocytic cells in the submucosal tissue (29, 30). Increased biofilm production is associated with bacterial persistence in CF patients (31) and mutations selected for during chronic infections in CF patients mirror those

4

observed during biofilm directed evolution experiments (32). The ability to form biofilms in Bcc, as well as the expression of multiple virulence factors, is controlled by numerous quorum sensing (QS) systems (33). A key class of QS systems associated with Bcc virulence are based on homoserine lactones (HSL) (24). Across the Bcc, some HSL QS systems are variable or lineage-specific, such as cciR/I and CepR2 (34, 35), while others are highly conserved in all members. One such highly conserved HSL QS system is the CepR/I regulon (36, 37), which generates N-octanoylhomoserine lactone (C8-HSL) using the HSL synthase CepI that in turns activates the transcriptional regulator CepR (37, 38). CepR is a major regulator of biofilm formation (39), and disruption of CepR/I attenuate Bcc virulence in several models (40, 41) and reduces disease severity (40, 42). The importance of the CepR/I QS system in Bcc virulence stems from its broad regulatory profile affecting multiple virulence-associated genes (43-45) such as those encoding the secreted zinc metalloproteases ZmpA (46) and ZmpB (47), siderophore production (39, 48) and the key mediator of Biofilm formation protein A (BapA) (45).

Glycosylation is increasingly recognised as a common modification in bacterial systems (49-56). Many glycosylation systems are conserved across bacterial genera (57, 58) and phyla (59, 60), suggesting glycosylation is critical for optimal proteome functionality. Disruption of glycosylation pathways in several species results in reduced fitness compared to glycosylation competent strains (52-56). However, the underlying cause of the reduction in fitness remains poorly defined (61, 62). Only recently have mechanistic insights emerged on how the loss of glycosylation affects bacterial physiology and pathogenesis. In *Campylobacter jejuni*, the loss of glycosylation results in decreased stability of the majority of known glycoproteins, which in turn affects virulence (63, 64). These data support a model whereby bacterial *N*-linked glycosylation contributes to protein stability, but it is unclear whether other glycosylation systems, such as *O*-linked glycosylation, have evolved to stabilize glycosylated proteins.

5

Previously, we reported *B. cenocepacia* possesses an *O*-linked glycosylation system responsible for the modification of at least 23 proteins with a trisaccharide glycan using the enzyme PglL (BCAL0960) (56). Building on this work we recently identified the biosynthetic locus, the <u>*O*</u>-<u>g</u>lycosylation <u>c</u>luster (OGC, BCAL3114 to BCAL3118) responsible for the generation of the *O*-linked glycan, established the *O*-linked glycan structure as β-Gal-(1,3)-α-GalNAc-(1,3)-β-GalNAc, and demonstrated that glycosylation was required for optimal bacterial fitness and resistance to clearance in *Galleria mellonella* infection models (65). Although these studies have demonstrated a link between glycosylation and virulence, the mechanism remains unclear. Using quantitative proteomic approaches, we sought to understand the proteome changes resulting from the loss of *O*-linked glycosylation in *B. cenocepacia*. We demonstrated that loss of glycosylation in *B. cenocepacia* resulted in global proteome alterations beyond the known glycoproteome, which are associated with widespread alterations in transcriptional regulation. We discovered that the HSL QS system CepR/I is repressed in glycosylation-defective mutants, which leads to defective biofilm formation and reduced siderophore production. In contrast to the loss of glycosylation in *C. jejuni,* we also demonstrate that only a few glycoproteins are reduced in abundance in the absence of glycosylation, but they are not responsible for the glycosylation-null phenotypes. Together, our data indicate that the roles of glycosylation in *B. cenocepacia* extend beyond protein stabilisation, and loss of *O*-linked glycosylation in *B. cenocepacia* causes dramatic physiological changes by altering the global regulatory CepR/I QS system.

Methods

Bacterial strains and growth conditions: Strains and plasmids used in this study are listed in Supplementary Table 1 and 2, respectively. Strains of *Escherichia coli* and *B. cenocepacia* were grown at 37°C in Luria-Bertani (LB) medium. When required, antibiotics were added to a final concentration of: 50 µg/ml trimethoprim for *E. coli* and 100 µg/ml for *B. cenocepacia*, 20 µg/ml tetracycline for *E. coli* and 150 µg/ml for *B. cenocepacia* and 40 µg/ml kanamycin for *E. coli*. Ampicillin was used at 100 µg/ml and polymyxin B at 25 µg/ml for triparental mating to select against donor and helper *E. coli* strains. Antibiotics were purchased from Thermo Fisher Scientific while all other chemicals unless otherwise stated were provided by Sigma-Aldrich.

Recombinant DNA methods. Oligonucleotides used in this study are listed in Supplementary Table 3. DNA ligations, restriction endonuclease digestions, and agarose gel electrophoresis were performed using standard molecular biology techniques (66) with Gibson assembly undertaken according to published protocols (67). All restriction enzymes, T4 DNA ligase and Gibson master mix were used as recommended by the manufacturer (New England Biolabs). *E. coli* pir2 and DH5α cells were transformed using heat shock-based transformation. PCR amplifications were carried out using either Phusion DNA (Thermo Fisher Scientific) or Pfu ultra II (Agilent) polymerases were used according to the manufacturer recommendations with the addition of 2.5% DMSO for the amplification of *B. cenocepacia* DNA due to its high GC content. DNA isolation, PCR recoveries and restriction digest purifications were performed using the genomic DNA clean-up kit (Zmyo research, CA) or Wizard SV gel and PCR clean-up system (Promega). Colony and screening PCRs were performed using GOTAQ Taq polymerase (Qiagen) supplemented with 10% DMSO when screening *B. cenocepacia*. DNA sequencing was undertaken at the Australian Genome Research Facility (Melbourne, Australia).

Construction of unmarked deletion mutants, endogenous tagged BCAL1086 and complementation with *pglL-his$_{10}$*. Deletions and endogenous tagging of BCAL1086 were

undertaken using the approach of Flannagan *et al.* for the construction of unmarked, non-polar deletions in *B. cenocepacia* K56-2 (68). Chromosomal complements of *pglL* were generated by introducing *pglL-his$_{10}$* under control of the *B. cenocepacia* S7 promoter (P_{S7}) or the native pglL promoter (Ppgl, 660bp upstream of PglL) inserted into *amrAB* using the pMH447 (23) derivative plasmids (Supplementary Table 2) according to the protocol of Aubert *et al* (69).

Protein manipulation and immunoblotting. Bacterial whole-cell lysates were prepared from overnight LB cultures of *B. cenocepacia* strains. 1ml of bacteria at an OD$_{600}$ of 1.0 were pelleted, then resuspended in 4% sodium dodecyl sulfate (SDS), 100 mM Tris pH 8.0, 20 mM dithiothreitol (DTT) and boiled at 95˚C with shaking at 2000 rpm for 10 minutes. Samples were then mixed with Laemmli loading buffer [24.8 mM Tris, 10 mM glycerol, 0.5% (w/v) SDS, 3.6 mM β-mercaptoethanol and 0.001% (w/v) of bromophenol blue (pH 6.8) final concentration] and heated for a further 5 minutes at 95°C. Lysates were then subjected to SDS PAGE using pre-cast 4-12% gels (Invitrogen) and transferred to nitrocellulose membranes. Membranes were blocked for 1 hour in 5% skim milk in TBS-T (20 mM Tris, 150 mM NaCl and 0.1% Tween 20) and then incubated for at least 16 hours at 4°C with either mouse monoclonal anti-His (1:2,000; AD1.1.10, AbD Serotech) or mouse anti-RNA pol (1:5,000; 4RA2, Neoclone). Proteins were detected using anti-mouse IgG horseradish peroxidase (HRP)-conjugated secondary antibodies (1:3,000; catalog number NEF822001EA, Perkin-Elmer) and developed with Clarity Western ECL Substrate (BioRad). All antibodies were diluted in TBS-T with 1% bovine serum albumin (BSA; Sigma-Aldrich). Images were obtained using an MFChemiBis imaging station (DNR Bio-Imaging Systems) or an Amersham imager 600 (GE life sciences).

Whole cell lysis of bacterial samples. Bacteria were grown overnight on LB plates. Plates were flooded with 5 ml of pre-chilled sterile phosphate-buffered saline (PBS) and colonies removed with a cell scraper. Cells were washed 3 times in PBS and collected by centrifugation at 10,000 x g at 4˚C then snap frozen. Frozen whole cell samples were

8

resuspended in 4% SDS, 100 mM Tris pH 8.0, 20 mM DTT and boiled at 95°C with shaking at 2000 rpm for 10 minutes. Samples were then clarified by centrifugation at 17,000 x g for 10 minutes, the supernatant collected, and protein concentration determined by bicinchoninic acid assay (Thermo Scientific Pierce). 200 μg of protein from each sample was acetone precipitated by mixing 4 volumes of ice-cold acetone with one volume of sample. Samples were precipitated overnight at -20°C and then centrifuged at 16,000 x g for 10 minutes at 0°C. The precipitated protein pellets were then resuspended in 80% ice-cold acetone and precipitated at -20°C. for an additional 4 hours. Samples were spun down at 17,000 x g for 10 minutes at 0°C to collect precipitated protein, the supernatant discarded, and excess acetone evaporated at 65°C for 5 minutes.

Enrichment of DNA bound proteins. Bacteria were grown and washed as above then tumbled for 20 minutes at room temperature in 1% formaldehyde in PBS in accordance with the protocol of Qin *et al* (70). Cross-linking was quenched with 125 mM (final concentration) glycine in PBS for 5 minutes with tumbling. Cells were collected and washed twice with ice-cold PBS and then DNA isolated using a Zymo genomic DNA clean-up kit according to the manufacturer's instructions with the exception of the DNA elution. DNA elution and reversal of DNA-protein cross-linking was undertaken by incubating the column at 68°C for 1 hour with protein elution buffer (2% SDS, 0.5 M β-mercaptoethanol and 300 mM Tris pH 8.5) according to Déjardin *et al* (71). Eluted proteins were collected by centrifugation and acetone precipitated by mixing 4 volumes of ice-cold acetone with one volume of sample. Samples were precipitated overnight at -20°C and then spun down at 16,000 x g for 10 minutes at 0°C. The precipitated protein pellets were precipitated with 80% ice-cold acetone and resuspended as indicated above.

Peptidomic analysis of bacterial samples. Bacterial strains were grown and washed as above then solubilized by boiling in guanidinium chloride lysis buffer (6 M GdmCl, 100 mM Tris pH 8.5, 10 mM tris(2-carboxyethyl)phosphine, 40 mM 2-chloroacetamide) according to the protocol of Humphrey *et al* (72). Peptidomic samples were isolated according to Parker *et al* (73). Briefly, guanidinium chloride lysis buffer solubilised lysates were precipitated with 20%

trichloroacetic acid on ice for 3 hours, then sample were centrifuged at 10,000 x g for 10 minutes at 0°C, the resulting supernatant collected and peptide isolated with tC18 columns (Waters). Bound peptides were eluted with 50% acetonitrile (ACN), 0.1% FA, dried and stored at -20°C.

Digestion of complex protein lysates. Dried protein pellets were resuspended in 6 M urea, 2 M thiourea, 40 mM NH_4HCO_3 and reduced / alkylated prior to digestion with Lys-C (1/200 w/w) then trypsin (1/50 w/w) overnight as previously described (74). Digested samples were acidified to a final concentration of 0.5% formic acid and desalted with home-made high-capacity StageTips composed on 5 mg Empore™ C18 material (3M, Maplewood, Minnesota) and 5 mg of OLIGO R3 reverse phase resin (Thermo Fisher Scientific) according to the protocol of Ishihama and Rappsilber (75, 76). Bound peptides were eluted with Buffer B (80% ACN, 0.1% FA), dried and stored at -20°C.

Reversed phase LC-MS. Purified peptides were resuspended in Buffer A* (2% ACN, 0.1% trifluoroacetic acid) and separated using a two-column chromatography set up comprising a PepMap100 C18 20 mm x 75 μm trap and a PepMap C18 500mm x 75μm analytical column (Thermo Scientific). Samples were concentrated onto the trap column at 5 μl/minute with Buffer A (2% ACN, 0.1%FA) for 5 minutes and infused into either an Orbitrap Elite™ Mass Spectrometer (Thermo Scientific), an Orbitrap Fusion Lumos Tribrid™ Mass Spectrometer (Thermo Scientific) or an Q-exactive plus™ Mass Spectrometer (Thermo Scientific) at 300 nl/minute via the analytical column using an Dionex Ultimate 3000 UPLC (Thermo Scientific). For whole cell proteomics analysis on the Orbitrap Elite™ 210 minute gradients were run altering the buffer composition from 1% buffer B to 28% B over 180 minutes, then from 28% B to 40% B over 10 minutes, then from 40% B to 100% B over 2 minutes, the composition was held at 100% B for 3 minutes, and then dropped to 3% B over 5 minutes and held at 3% B for another 10 minutes. The Orbitrap Elite™ was operated in a data-dependent mode automatically switching between the acquisition of a single Orbitrap MS scan (60,000 resolution) followed by 5 data-dependent HCD MS-MS events (resolution 15 k

10

AGC target of 4 x 10^5 with a maximum injection time of 250 ms, NCE 35) with 30 seconds dynamic exclusion enabled. For whole cell proteomics analysis on the Fusion™ 120 minute gradients were run altering the buffer composition from 1% buffer B to 28% B over 90 minutes, then from 28% B to 40% B over 10 minutes, then from 40% B to 100% B over 2 minutes, the composition was held at 100% B for 3 minutes, and then dropped to 3% B over 5 minutes and held at 3% B for another 10 minutes. The Fusion™ was operated in a data-dependent acquisition switching between the acquisition of an Orbitrap MS scan (120,000 resolution) every 3 seconds and HCD undertaken for each selected precursor (maximum fill time 100 ms, AGC 5 x 10^4 with a resolution of 15,000 for Orbitrap MS-MS scans) with 30 seconds dynamic exclusion enabled.

DNA bound proteomic analysis was undertaken on both a Orbitrap Elite™ (for data-dependent acquisition experiments) and Q-exactive plus™ (for data-independent acquisition experiments) with 90 minute gradients run altering the buffer composition from 1% buffer B to 28% B over 60 minutes, then from 28% B to 40% B over 10 minutes, then from 40% B to 100% B over 2 minutes, the composition was held at 100% B for 3 minutes, and then dropped to 3% B over 5 minutes and held at 3% B for another 10 minutes. For data-dependent acquisition experiments the Elite™ Mass Spectrometer was operated in a data-dependent mode automatically switching between the acquisition of a single Orbitrap MS scan (60,000 resolution) followed by 10 data-dependent CID MS-MS events (analysed within the ITMS, maximum injection time of 100 ms, NCE 35). To enable the robust quantification of CepR data-independent acquisition was undertaken using parallel reaction monitoring (PRM (77)) monitoring tryptic peptides of BCAL3530 (DNA-binding protein HU-alpha), BCAL0462 (Putative DNA topoisomerase III), BCAM0904 (DNA polymerase I), BCAM1868 (CepR) and BCAM1870 (CepI), Supplementary Table 4. BCAL3530, BCAL0462, BCAM0904 were included as positive controls to ensure equal DNA enrichment while CepI is a non-DNA binding control. Data-independent acquisition was performed by switching between the acquisition of a single Orbitrap MS scan (70,000 resolution, m/z 350-1400) and HCD MS/MS events of each

11

PRM precursor (maximum fill time 110ms, AGC 2 x 10^5 with a resolution of 35,000 for Orbitrap MS-MS scans, see Supplementary Table 4 for further details).

Peptidomic analysis was undertaken on an Orbitrap Elite™ with 120 minute gradients run altering the buffer composition from 1% buffer B to 28% B over 90 minutes, then from 28% B to 40% B over 10 minutes, then from 40% B to 100% B over 2 minutes, the composition was held at 100% B for 3 minutes, and then dropped to 3% B over 5 minutes and held at 3% B for another 10 minutes. The Elite™ Mass Spectrometer was operated in a data-dependent mode automatically switching between the acquisition of a single Orbitrap MS scan (60,000 resolution) followed by 5 data-dependent CID and HCD MS-MS events (both acquired within the Orbitrap for each precursor at a resolution of 15 k AGC target of 4 x 10^5 with a maximum injection time of 250 ms, NCE 35) with 30 seconds dynamic exclusion enabled.

Data analysis: MS datasets were processed using MaxQuant (v1.5.5.1 or 1.5.3.30 (78)). Database searching was carried out against the reference *B. cenocepacia* strain J2315 (https://www.uniprot.org/proteomes/UP000001035, downloaded September 25th 2017) and the K56-2Valvano proteome (79) (http://www.uniprot.org/taxonomy/985076, downloaded from NCBI February 15th 2013). All tryptic digest searchers were undertaken using "Trypsin" enzyme specificity, carbamidomethylation of cysteine as a fixed modification; oxidation of methionine, acetylation of protein N-terminal trypsin/P cleavage with a maximum of 2 missed cleavages. Peptidomic analysis was undertaken using "Unspecific" enzyme specificity and allowing the presence of *O*-linked glycosylation BC glycan 1 (elemental composition: $C_{22}O_{15}H_{36}N_2$, mass: 568.2115) and BC glycan 2 (elemental composition: $C_{26}O_{18}H_{40}N_2$, mass: 668.2276) at serine residues. To enhance the identification of peptides between samples, the Match between Runs option was enabled with a precursor match window set to 2 minutes and an alignment window of 10 minutes. For label free quantitation the MaxLFQ option in Maxquant (80) was enabled in addition to the re-quantification module. The resulting outputs were processed within the Perseus (v1.5.0.9) (81) analysis environment to remove reverse matches and common protein contaminates prior to further analysis. For label-free based

quantitative (LFQ) comparisons missing values were imputed using Perseus and data z-scored to enabled visualization in heat maps using R (https://www.r-project.org/). Pearson correlations were performed on non-imputed dataset with clustering and visualization performed in Perseus. Clustering of Pearson correlations data was undertaken using the Euclidean distance and complete linkage with pre-processing with k-means in Perseus. Enrichment analysis was undertaken using Fisher exact test in Perseus with Gene Ontology (GO) terms, gene names, subcellular location [CC], signal peptide status, lipidation status, intramembrane status and keywords associated with each protein obtain from uniport (*B. cenocepacia* strain J2315 proteomes: UP000001035, downloaded September 25th 2017). Virulence associated genes were compiled from genes defined as Virulence associated within the *Burkholderia* Genome Database (82) (J2315, Downloaded 3rd October 2017) and the genome analysis of *B. cenocepacia* strain J2315 (83) (Supplementary Table 6). CepR regulated proteins were defined as those proteins which were previously reported by O'Grady *et al* as differential regulated in K56-2 Δ*cepR* at stationary phase (43). Proteomics data sets have been deposited to the ProteomeXchange Consortium via the PRIDE (84) partner repository with the dataset identifier PXD014429, PXD014516, PXD014581, PXD014614 and PXD014700. For a complete description of each PRIDE dataset see Supplementary Table 5.

Motility assays. Motility assays were conducted using semi-solid motility agar consisting of LB infusion medium supplemented with 0.3 % agar as previously described (56). Plates were inoculated using 2 µl of standardized, OD_{600} of 0.5, overnight cultures of each strain. Motility zones were measured after 48 hour incubation at 37°C. Experiments were carried out in triplicate with 3 biological replicates of each strain.

Transcriptional Analysis by luminescence assays. To assess transcriptional changes in CepR and CepI *luxCDABE* reporter assays were performed using *B. cenocepacia* K56-2 wild-type (WT), Δ*pglL*, Δ*OGC* and Δ*pglL amrAB::S7-pglL-his*$_{10}$ strains containing pCP300 (CepI promoter *luxCDABE* reporter (85)), pPromcepR (CepR promoter *luxCDABE* reporter (86)) or pMS402 (promoterless *luxCDABE* reporter (87)) as a negative control.

13

Overnight cultures were diluted to an OD_{600} of 1.0 and 2 μl inoculated into 200 μl LB supplemented with 100 μg/ml trimethoprim in black, clear-bottomed 96-well microplates (minimum of eight technical replicates per independent biological replicate). The OD_{600} and relative luminescence were measured using a CLARIOstar plate reader at 10-minute intervals for 24 hours. Experiments assessing the effect of C_8-HSL additions on CepR and CepI transcription were performed according to Le Guillouzer *et al* (88). Briefly, cultures were supplemented with C_8-HSL (Sigma-Aldrich) resuspended in acetonitrile (10 μM final concentration) and added to cultures with acetonitrile added alone used as a negative control. Plates were incubated at 37°C with shaking at 200 rpm between measurements with each assay undertaken 3 independent times on separate days. The resulting outputs were visualised using R (https://www.r-project.org/).

Biofilm Assay. Biofilm assays were performed according to previous reports (26, 89, 90) using protocols based on the approach of O'Toole (91). *B. cenocepacia* strains were grown overnight at 37°C and adjusted to an OD_{600} of 1.0. 10 μl of these suspensions were inoculated into 990 μl of LB supplemented with 0.5% (wt/vol) casamino acids and 100 μl added in to 96-well microtiter plates (Corning Life Sciences, minimum of eight technical replicates per independent biological replicate). Microtiter plates were incubated at 37°C for 24 hours in a closed humidified plastic container. The plates were then washed with PBS to remove planktonic cells then stained for 15 minutes with 125 μl of 1% (wt/vol) crystal violet. Excess crystal violet was removed with two washes of PBS and 200 μl of 33% (vol/vol) acetic acid was added for 15 minutes to release the stain. Resuspended stain was transferred to a new plate and measured on a CLARIOstar plate reader measuring the absorbance of the resulting solution at 595 nm. Three independent assays were undertaken on separate days.

***Galleria mellonella* infection assays.** Infection of *G. mellonella* larvae was undertaken using the approach of Seed and Dennis (92) with minor modifications. *B. cenocepacia* strains were grown overnight at 37°C and adjusted to an OD_{600} of 1.0, equivalent to 2×10^9 cfu/ml (colony-forming units / ml). Strains were diluted with PBS to 4×10^5 cfu/ml

14

with serial dilution plates undertaken to confirm inoculum levels. For each strain, 2000 cfu in 5 μl was injected in the right proleg of the *G. mellonella* larvae. 3 independent challenges were performed with each strain injected into 8 to 10 *G. mellonella* larvae. For each independent challenge 8 control larvae were injected with 5 μl PBS. Post infection *G. mellonella* larvae were placed in 12-well tissue culture plates and incubated in the dark at 30°C. The number of dead larvae was scored at 24, 48, and 72 hours after infection with death of the larvae determined by loss of responsiveness to touch. The results visualised using R (https://www.r-project.org/) and statistical analysis of survival curves undertaken with the survminer package (version 0.4.5).

CAS siderophores assays. Alterations in production of siderophores was assessed using Chrome Azurol S (CAS) assay as previously described (93, 94). 10 μl of OD_{600} 1.0 adjusted bacterial culture were spotted on CAS agar plates and incubated at 37°C for 24 hours. The diameter of the zone of discoloration from the removal of iron from the CAS dye complex was measured. Experiments were carried out in technical triplicate with 3 biological replicates.

Proteases activity-based probes. K56-2 WT, Δ*pglL* and Δ*pglL amrAB::S7-pglL-his*$_{10}$ strains were grown overnight on confluent LB plates. Plates were flooded with 5 ml of pre-chilled sterile PBS and colonies removed with a cell scraper. Cells were washed 3 times in chilled PBS and resuspend in 40 mM Tris, 150 mM NaCl pH 7.8 then lysed by sonication. Samples were clarified by centrifugation, 10,000 x g, 10 minutes at 4°C and samples were diluted to a total concentration of 4 mg/ml. Reactivity to three classes of activity-based probes were assessed using PK-DPP (Cy5-tagged probe for Trypsin-like proteases (95)), PK105b (Cy5-tagged probe for Elastase-like proteases (96)), PK101 (Biotin-tagged probe for Elastase-like proteases (97)) and FP-Biotin (Biotin-tagged probe for Serine hydrolases (98)) which were added at 1.3 μM from a 100x DMSO stock. Untreated control samples were prepared in parallel and left untreated to allow the assessment of autofluorescence and endogenous biotinylation in lysates. Samples were incubated at 37˚C for 15 minutes to allow labelling and

then quenched by the addition of Laemmli Sample Buffer. Samples were then boiled and proteins were resolved on a 15% SDS-PAGE gel. For Cy5-tagged probes, labelling was detected by directly scanning the gel for Cy5 fluorescence using a Typhoon 5 flatbed laser scanner (GE Healthcare). For FP-Biotin, proteins were transferred to nitrocellulose and the membrane was incubated with streptavidin-AlexaFluor647 at 4°C overnight. Following three washes with PBS containing 0.05% Tween 20, the membrane was scanned on the Typhoon 5 in the Cy5 channel. Experiments were carried out in biological triplicate. All probes were synthesised in house by the Edgington-Mitchell Laboratory according to published methods, with the exception of FP-Biotin, which was purchased from Santa Cruz Biotechnology.

Results

Loss of glycosylation in *B. cenocepacia* leads to global proteome alterations.

We previously demonstrated that loss of glycosylation causes defects in motility (56), reduction of virulence in plant and insect infection models (56, 65), and defects in carbon utilisation (65). To better understand the role of glycosylation in *B. cenocepacia* we assessed the effect of loss of glycosylation on the proteome. To achieve this we generated markerless deletion mutants in the *O*-oligosaccharyltransferase *pglL (ΔpglL*; BCAL0960 (56)) gene, the recently identified *O*-linked glycan cluster *(ΔOGC*; BCAL3114 to BCAL3118) responsible for the generation of the glycan used for *O*-linked glycosylation (65), and a double glycosylation null strain *(ΔpglLΔOGC*). We also constructed a chromosomal *pglL* complemented strain *(ΔpglL amrAB::S7-pglL-his₁₀*, Supplementary Figure 1A). The rationale for creating multiple glycosylation-defective strains was to eliminate potential confounding effects arising from blocking glycosylation at a specific step and the corresponding accumulation of unprocessed lipid-linked glycans. Western blot analysis using the glycoprotein acceptor protein DsbA$_{Nm}$-his$_6$ (56, 99) confirmed the loss of glycosylation in *ΔpglL*, *ΔOGC*, and *ΔpglLΔOGC*, as well as restoration of glycosylation in *ΔpglL amrAB::S7-pglL-his₁₀* (Figure 1A). In contrast to our previously reported plasmid based PglL complementation approaches (56) chromosomal complementation lead to the restoration of glycosylation to near wild-type levels (Supplementary Figure 1B) as well as restoration of motility (Supplementary Figure 1C) compared to only partial restoration previously reported (56).

Using label-free based quantitative proteomics, 5 biological replicates of each strain were investigated leading to the identification of 3399 proteins with 2759 proteins quantified in at least 3 biological replicates in a single biological group (Supplementary Figure 2, Supplementary Table 7). Hierarchical clustering of Pearson correlations of proteome samples demonstrated robust correlation between all samples (Average Pearson correlation of 0.98, Supplementary table 8) yet three discrete proteome clusters were readily identified separating the wild-type K56-2, *ΔpglL amrAB::S7-pglL-his₁₀* strains and glycosylation-null strains (Figure

17

1B). Examination of the most profound alterations, proteins with $-\log_{10}(p)>3$ and a fold change greater than +/- 2 $\log_2$ units, revealed alterations in protein levels observed in $\Delta pglL$ that were mirrored in strains ΔOGC and $\Delta pglL\Delta OGC$, which were restored by complementation (Figure 1C). Consistent with the observed motility defects (Supplementary Figure 1C), the levels of proteins associated with flagella-mediated motility and chemotaxis, including BCAL0114 (FliC), BCAL0129 (CheA), BCAL0524 (FliG) and BCAL0525 (FliF), were significantly reduced in glycosylation-null strains. Importantly, multiple known virulence-associated proteins were also decreased in the glycosylation-null strains including the heme receptor protein BCAM2626 (HuvA (100)) and nematocidal protein BCAS0293 (AidA (101)). Numeration of the overlap of all altered protein between glycosylation-null strains by Fisher exact enrichment analysis demonstrated a substantial enrichment between these three groups (Fisher exact test: 6.7502 x 10^{177} and 4.3784 x 10^{245} for $\Delta pglL$ compared with ΔOGC, and for $\Delta pglL$ compared with $\Delta pglL\Delta OGC$, respectively, Supplementary Table 9, Supplementary Figure 3). These results revealed that the loss of glycosylation due to disruption of *pglL* or *OGC* leads to similar changes, which are largely complemented to parental levels by reintroduction of *pglL* in the chromosome.

Loss of glycosylation results in reduced CepR/I transcription and the levels of DNA associated CepR. Enrichment analysis of the altered proteins within glycosylation-null strains demonstrate the over representation of a range of categorical groups based on GO terms, protein localization and virulence associated factors assignments. These groups highlight that protein localizations assignments and virulence associated factors were similarly affected in $\Delta pglL$ and ΔOGC, recapitulating observations made at the individual protein level (Figure 2, Supplementary Table 9). Interestingly, enrichment analysis highlighted the link between the loss of *O*-linked glycosylation and changes that were broader than only motility and virulence. For example, differences also observed in proteins associated with DNA-sequence specific binding and transcriptional regulation (Figure 2, Supplementary Table 9). This observation suggested that the loss of glycosylation results in alterations in the

transcriptional landscape of *B. cenocepacia*. As virulence is coordinated by global regulators such as CciR, CepR, ShvR and AtsR in *B. cenocepacia* (35, 43, 86, 102), we assessed if known regulators could account for the observed proteome changes in glycosylation-null strains. As our data demonstrated minimal alteration of the regulator ShvR (BCAS0225, Supplementary Table 7) across the analysed strains, and disruption of both *atsR* (*BCAM0379*) and *cciR* (*BCAM0240*) has previously been associated with increased motility (43, 86), we reasoned that the regulator CepR may be responsible for the glycosylation-dependent differences in our mutant strains. This would be consistent with the observed decrease in BCAS0293 (AidA, Figure 1C) which is stringently regulated by CepR (45, 103). Using available microarray data of CepR-regulated genes (43), we investigated the correlation of the proteome changes observed in the absence of glycosylation, with alterations observed in response to the disruption of CepR. We observed a statistically significant enrichment of CepR-regulated proteins altered in the absence of glycosylation (multiple hypothesis corrected *p*-value 1.79 x 10^6 and 6.69 x 10^6 for $\Delta pglL$ and ΔOGC respectively, Supplementary table 9), supporting a link between CepR and the alteration observed in glycosylation-null strains and suggesting that the loss of glycosylation may influence the *B. cenocepacia* CepR regulon.

To determine transcriptional changes in *cepR/I* genes we introduced the *cepR* and *cepI* luciferase promoter reporter (pPromcepR (86) and pCP300 (85)) into wild-type K56-2, $\Delta pglL$ and $\Delta pglL$ *amrAB::S7-pglL-his₁₀*. Consistent with our proteomic results, $\Delta pglL$ showed decreased induction of both *cepI* and *cepR* over a 24-hour period (Figure 3A, Supplementary Figure 4) compared with wild type and $\Delta pglL$ *amrAB::S7-pglL-his₁₀*. Detailed examination at 12 hours (log phase), 16 hours (the transition from log to stationary phase) and 20 hours (stationary phase) revealed higher levels of transcription in the wild type of both *cepI* and *cepR* at 16 and 20 hours compared with transcription levels in $\Delta pglL$, despite comparable growth kinetics (Supplementary Figure 5). As the C8-HSL levels affect the response of CepI and CepR in *B. cenocepacia* (39, 44, 104), we assayed *cepR/I* transcription in the absence and presence of additional C8-HSL (10 μM, Figure 3B). In response to exogenous C8-HSL, *cepI*

transcription increased in all strains (Figure 3B), consistent with the positive feedback response expected to heighten C8-HSL levels (39, 44). In contrast, while the addition of C8-HSL led to no change in *cepR* transcription in Δ*pglL*, it resulted in reduced transcription of *cepR* to the level observed in the wild type K56-2. As expected from the reduction in *cepR/I* transcription resulting from the loss of glycosylation, *cepR* and *cepI* transcription was also compromised in Δ*OGC* strains (Supplementary Figure 6 and 7). Together, these results indicate that both *cepR* and *cepI* transcription are altered in the loss of glycosylation, with the resulting *cepR* levels resembling the levels observed during C8-HSL-induced repression in wild type.

As the CepR protein autoregulates *cepR*'s own transcription (48), we reasoned that the decreased transcription in Δ*pglL* would correspond to decreased levels of DNA bound CepR. To directly assay DNA binding by CepR, we monitored the DNA bound proteome using formaldehyde-based cross-linking coupled to DNA enrichment (105). Initial analysis of the DNA-bound proteome found glycosylation-null strains (Δ*pglL* and Δ*OGC*) and glycosylation-proficient strains (wild type and Δ*pglL armAB::S7-pglL-his*$_{10}$) possessed distinct proteome profiles with multiple uncharacterised transcriptional regulators (e.g. BCAL0946, BCAL1916, BCAS0168, BCAL2309 and BCAL0472) which were altered by the loss of glycosylation (Figure 3C, Supplementary Table 10). Although this analysis enabled the identification of CepR, its low abundance prevented its quantitation across biological replicates. To improve the monitoring of CepR, targeted proteomic analysis was undertakening using PRM assays confirming the reduction in DNA associated CepR in Δ*pglL* compared with wild type and Δ*pglL armAB::S7-pglL-his*$_{10}$ (Figure 3D, *p*-value= 0.017 wild type vs ΔpglL, Supplementary Table 11). In agreement with the total proteome and *lux* reporter measurements, the DNA-bound proteome supports multiple transcription associated proteins, including the global regulator CepR, that are altered in the absence of glycosylation.

Δ*pglL* demonstrates a reduced ability to form biofilms and produce siderophores. The observed reductions in CepR/I transcription suggested that CepR/I-linked regulation may also be altered in glycosylation-null strains. To test this hypothesis, we assessed two phenotypes associated with CepR/I regulation, the production of biofilm under static 24-hour growth and siderophore production (39, 43-45, 48). Consistent with an impact of glycosylation on CepR/I-mediated regulation, we observed a profound reduction in biofilm formation in Δ*pglL*, which was partially restored by complementation (Figure 4A). Interestingly, we observed that the method of complementation, i.e. expression of PglL-his$_{10}$ driven from the native pglL promoter (Δ*pglL amrAB::native-pglL-his$_{10}$*) or from the constitutive S7 promoter (Δ*pglL amrAB::S7-pglL-his$_{10}$*) impacted the restoration of biofilm formation (Figure 4A). Examination of independently created Δ*pglL* and Δ*pglL amrAB::native-pglL-his$_{10}$* strains confirmed a link between biofilm formation, through phenotype restoration following complementation (Supplementary Figure 8). CAS assays, used to assess the global levels of siderophore activity, demonstrated a modest but reproducible effect in Δ*pglL* which was completely restored by complementation when PglL was expressed from either the native or S7 promoter (Figure 4B and C). Together, these findings support the notion that CepR/I regulate multiple phenotypes including biofilm and siderophore production, which are affected by the loss of glycosylation.

Except for BCAL1086 and BCAL2974, proteins that are normally glycosylated remain stable in the absence of glycosylation. As the loss of glycosylation in other bacterial glycosylation systems leads to protein instability (63, 64, 106), we examined whether protein instability in *B. cenocepacia* may be responsible for the phenotypic changes in glycosylation-null strains. Our proteomic analysis identified 21 out of 23 known glycoproteins (56), yet only 2 were altered in abundance in glycosylation-negative strains; BCAL1086 (-5.7 log$_2$) and BCAL2974 (-2.5 log$_2$) (Figure 5A, Supplementary Table 7). To confirm the observed decreases in abundance, endogenous BCAL1086 and BCAL2974 were his$_{10}$-tagged at the C'-terminus. While his-tagging did not allow the detection of BCAL2974 by western analysis

21

(data not shown), the introduction of the his_{10} epitope into BCAL1086 allowed quantification of endogenous BCAL1086 in the K56-2 wild-type, $\Delta pglL$ and $\Delta pglL$ $amrAB::S7\text{-}pglL\text{-}his_{10}$ backgrounds and confirmed the loss of BCAL1086 in $\Delta pglL$ (Figure 5B). We sought to directly assess whether BCAL1086 was subjected to increased degradation in $\Delta pglL$, as a measure of instability. For this, we monitored the endogenous peptide pool (73) quantifying peptides derived from 783 proteins (Supplementary Table 12 and 13) in *B. cenocepacia* K56-2 WT, $\Delta pglL$ and $\Delta pglL$ $amrAB::S7\text{-}pglL\text{-}his_{10}$ strains. Consistent with the degradation of BCAL1086 we observed an increase in the abundance of BCAL1086-derived peptides in $\Delta pglL$ while peptides from other known glycoproteins showed only modest changes (Figure 5C, Supplementary Table 13). Within this peptidomic analysis, we observed that multiple unique BCAL1086 peptides are were present in $\Delta pglL$ clustered around the central region of BCAL1086 (Figure 5D), confirming that BCAL1086 was expressed in $\Delta pglL$ but was subject to proteolysis. Together, our data support that BCAL1086 becomes degraded in the absence of glycosylation, but the majority of known *B. cenocepacia* glycoproteins are unaffected.

Role of BCAL1086 and BCAL2974 in $\Delta pglL$ phenotypes. As changes in the glycoproteins BCAL2974 and BCAL1086 coincided with an alteration in CepR/I activity, we investigated if the loss of BCAL2974 and BCAL1086 could be responsible for defects observed in $\Delta pglL$. To answer this question, $\Delta BCAL2974$ and $\Delta BCAL1086$ strains were created and assessed for their effect on biofilm and siderophore production as well as virulence in *G. mellonella*, a phenotype previously associated with $\Delta pglL$ (56). Assessment of 24-hour static biofilm growth showed $\Delta BCAL1086$ had no effect on biofilm formation while $\Delta BCAL2974$ resulted in a small but consistent decrease in biofilm development. However, this effect is minimal compared to the defect observed in $\Delta pglL$ and $\Delta cepI$ (Figure 6A). The ability of $\Delta BCAL1086$ and $\Delta BCAL2974$ to produce siderophores was unaffected (Figure 6B and C). Similarly, while *G. mellonella* infections showed that $\Delta pglL$ causes reduced mortality at 48 hours post infection compared to K56-2 WT, (p-value 0.0015), $\Delta BCAL2974$, $\Delta BCAL1086$ and $\Delta pglL$ $amrAB::native\text{-}pglL\text{-}his_{10}$ strains resulted in wild type levels of lethality in *G. mellonella*

22

at 48 hours (Figure 6D). These results suggest that even though BCAL2974 and BCAL1086 are influenced by the loss of glycosylation, neither protein is solely responsible for the known defect observed in ΔpglL.

We also investigated whether the loss of either BCAL2974 or BCAL1086 drives proteome changes. Using label-free based quantitative proteomics we compared the proteomes of K56-2 WT, *ΔBCAL2974*, *ΔBCAL1086*, *ΔpglL*, *ΔcepR*, *ΔcepI* and *ΔpglL amrAB::S7-pglL-his$_{10}$* to assess the similarity between the proteomes as well as the specific proteins effected by the loss of these proteins. Proteomics analysis led to the identification of 3730 proteins with 2752 proteins quantified in at least 3 biological replicates in a single biological group (Supplementary Table 14). Clustering of the proteomic analysis revealed that *ΔBCAL2974* and *ΔBCAL1086* closely grouped with that of WT strains while, *ΔpglL*, *ΔcepR*, *ΔcepI* and *ΔpglL amrAB::S7-pglL-his$_{10}$* formed discrete clusters. This macro analysis indicated that mutations in BCAL2974 or BCAL1086 had a minimal effect on the proteome (Figure 7A, Supplementary Table 15A and B). Consistent with this conclusion, analysis of the specific proteins that varied between the different strains demonstrated few proteome alterations in *ΔBCAL2974* and *ΔBCAL1086* compared with *ΔpglL*, *ΔcepR* and *ΔcepI* (Figure 7B) with *ΔcepR*, *ΔcepI* and *ΔpglL* also demonstrating the expected similarility in their proteome changes (Fisher exact test *ΔcepR* vs *ΔpglL*, *p*-value 3.25 x 10^5 and *ΔcepI* vs *ΔpglL*, 6.95 x 10^4, Supplementary Table 16). Taken together the proteome analysis supports the contention that BCAL2974 and BCAL1086 have minimal effect on the proteome and are not responsible for the broad proteomic alterations observed in *ΔpglL*.

Discussion

Although glycosylation is a common protein modification in bacterial species (49-51, 107) our understanding of how this modification influences bacterial physiology and pathogenesis is unclear. Recent insights into how glycosylation impacts bacterial proteomes have been obtained through study of the archetypical *N*-linked glycosylation system of *C. jejuni* (108, 109), yet it is unclear whether these observations are generalizable to another glycosylation systems such as *O*-linked glycosylation systems. Studies on the role of *N*-linked glycosylation within *C. jejuni* have revealed that defects associated with the loss of glycosylation stem from the loss of glycoproteins (108, 109) suggesting that *N*-linked glycosylation extends protein longevity in *C. jejuni*. In contrast, we find here that loss of *O*-linked glycosylation in *B. cenocepacia* has a more limited effect on the proteins targeted for glycosylation with only a subset of the known glycoproteins affected by the disruption of glycosylation (Figure 5). Therefore, the defect associated with loss of glycosylation in *B. cenocepacia* cannot be merely explained by protein instability. Indeed, we demonstrate that loss of glycosylation leads to changes in the expression of non-glycosylated proteins regulated by the CepR/I regulon (Figure 3), a global regulator of bacterial physiological changes including virulence and motility (39, 42, 48). Also consistent with a defect in the CepR/I regulon, loss of glycosylation results in lack of biofilm formation and reduced siderophore production. Therefore, our findings uncover a previously unknown link between loss of glycosylation and the repression of the CepR/I QS system.

The observation that biofilm formation is reduced in Δ*pglL* mirrors previous reports in *Acinetobacter baumannii* (55) and *C. jejuni* (63), but the link of this phenotype to alterations in regulations have not previously documented. Previous studies in *B. cenocepacia* have identified that not all CepR/I regulated proteins are required for biofilm formation. However, BapA (BCAM2143) plays a major role in the formation of biofilms on abiotic surfaces, whereas the lectin complex BclACB (BCAM0184–BCAM0186) contributes to biofilm structural development (45). Although BapA (BCAM2143) was not detected by our proteomic analysis,

BclA and BclB (BCAM0186 and BCAM0184 respectively) were observed and decreased in $\Delta pglL$ (both -1.0 log_2 decrease compared with WT, -log_{10}(p): >3.05, Supplementary Table 7). Surprisingly, BclA and BclB increased in abundance in $\Delta pglL\Delta OGC$ and ΔOGC strains (both 1.0 log_2 increase compared with WT, -log_{10}(p) >1.4, Supplementary Table 7), and these mutants formed extensive biofilms (Supplementary Figure 9). This result is consistent with recent work which has shown that with disruption of BCAL3116, the third gene in the OGC, resulted in enhanced biofilm formation (110) although the underlying mechanism driving this phenomenon is unclear. Concerning siderophore production, our proteomic data reveal that siderophore-associated proteins were reduced in both $\Delta pglL$ and ΔOGC (Figure 2) with glycosylation-null strains producing reduced zones of clearing in the CAS assays (Figure 4B and C, Supplementary Figure 10). However, the magnitude of the reduction in the CAS assays differed in the mutant since ΔOGC and $\Delta pglL\Delta OGC$ presented significantly smaller zones of clearing than $\Delta pglL$ (Supplementary Figure 10). These results highlight that although the proteome changes observed in the glycosylation mutants $\Delta pglL$ and ΔOGC are highly similar they are not identical and show phenotypic differences. Therefore, a key question arising from our findings is how the loss of glycosylation alters gene regulation and whether the observed defects are simply the result of altered CepR transcriptional control. The lack of any glycosylated QS-associated proteins in *B. cenocepacia* (56) makes the identification of the link between a specific glycoprotein and QS changes unclear.

It is possible the observed alterations in biofilm formation and siderophore production are not solely driven by altered CepR regulation, but also reflect additional transcriptional alterations in the glycosylation null strains. This conclusion agrees with our observations of many differences in the abundance of transcriptional regulators in the DNA-associated proteome of glycosylation null strains (Figure 3C, Supplementary Table 10). An additional driver of these pleotropic effects may also be deleterious outcomes resulting from the manipulation of the *O*-linked glycosylation system. It has been suggested in *C. jejuni* that the disruption of

glycosylation leads to undecaprenyl diphosphate decorated with *N*-linked glycan being sequestered from the general undecaprenyl diphosphate pool and that this depot effect may be a general phenomenon observed in all glycosylation mutants (64). Sequestration of undecaprenyl diphosphate was thought to drive an increase in the abundance of proteins within the non-mevalonate and undecaprenyl diphosphate biosynthesis pathways observed in glycosylation-null *C. jejuni* (64). However, in *B. cenocepacia* glycosylation mutants, we observe only minor alterations in the non-mevalonate (BCAL0802, BCAL1884, BCAL2015, BCAL2016, BCAL2085, BCAL2710, BCAM0911 and BCAM2738, Supplementary Figure 10A) and undecaprenyl diphosphate biosynthesis (BCAL2087 and BCAM2067, Supplementary Figure 10B) pathways, which argues against this phenomenon being common to all glycosylation mutants. Furthermore, the similarity of the proteome changes in the Δ*pglL*, Δ*OGC* and Δ*pglL*Δ*OGC* strains (Supplementary Figure 3) supports the conclusion that proteome changes are independent of the sequestration of the undecaprenyl diphosphate pool as Δ*OGC* and Δ*pglL*Δ*OGC* strains are unable build the *O*-linked glycan on undecaprenyl diphosphate.

Another explanation for the pleiotropic effects associated with loss of *O*-glycosylation could be the instability of the glycoproteins in the absence of the glycan. We identified two glycoproteins BCAL2974 and BCAL1086, both of unknown functions, which are reduced in abundance due to the loss of glycosylation. However, genetic experiments demonstrate that neither protein is responsible for the phenotypic and proteomic changes associated with loss of glycosylation (Figure 6 and 7). Further, in the case of BCAL1086, endogenous tagging and degradomic analysis confirm the loss of this protein in the Δ*pglL* background. Although these results support the breakdown of BCAL1086 as a consequence of the loss of glycosylation, an alternative explanation is that the changes in degradation arise from alterations in protease levels or activities in the Δ*pglL* mutant. Previously, we reported that Δ*pglL* results in enhanced casein proteolytic activity (65). However, our global proteome analysis shows only modest

26

changes in protease levels. We also observed identical protease profiles from activity probe against multiple classes of protease in wild type, $\Delta pglL$ and $\Delta pglL$ $amrAB::S7\text{-}pglL\text{-}his_{10}$ (Supplementary Figure 12), suggesting all of these strains have similar protease activities. More importantly, aside of glycoproteins BCAL2974 and BCAL1086, the other proteins targeted for glycosylation remain consistently stable in the glycosylation-defective mutants. Therefore, although loss of glycosylation may affect the stability of some glycoproteins, the pleiotropic effect found in the glycosylation mutants cannot be explained by alterations in protein degradation.

In summary, this work provides a global analysis of the impact of *O*-linked glycosylation on *B. cenocepacia* traits. The application of quantitative proteomics enabled the assessment of nearly half the predicted proteome of *B. cenocepacia* K56-2 and revealed a previously unknown link between *O*-linked glycosylation and the CepR/I regulon. The alteration in CepR transcription as well as its associated phenotypes support a model in which the virulence defects observed for glycosylation null strains arise from transcriptional changes and not from the direct result of glycosylation loss per se. This work challenges the idea that loss of glycosylation solely affects the stability and activity of the glycoproteome, and instead shows that glycosylation can influence the bacterial transcriptional profile and broader proteome.

27

Figure 1. Disruption of *O*-linked glycosylation results in multiple changes in the proteome. A) Western analysis of strains expressing the glycosylation substrate DsbA$_{Nm}$-his$_6$ confirms the loss of glycosylation in Δ*pglL*, Δ*OGC*, Δ*pglL*Δ*OGC* and restoration of glycosylation in the chromosomal complement Δ*pglL amrAB::S7-pglL-his$_{10}$*. B) Pearson correlation analysis demonstrate three discrete clusters observed across the proteomic analysis which separate glycosylation competent and glycosylation-null strains. C) Z-scored heatmap of proteins observed to undergo alterations between glycosylation-competent and glycosylation-null strains reveals alterations in motility and chemotaxis (proteins bolded) including BCAL0114 (FliC), BCAL0524 (FliG), BCAL0525 (FliF) as well as known CepR regulated protein BCAS0293 (AidA).

Figure 2. Heatmaps of glycosylation-null strains enrichment analysis. The multiple hypothesis corrected *p*-values from Fisher exact tests demonstrate proteins with similar GO terms, localisations and associated with virulence factors are altered with glycosylation-null strains.

Figure 3. CepR/I transcription are altered in glycosylation-null strains. A) 24-hour luciferase profile of strains grown with either the CepI reporter pCP300 or CepR reporter pPromCepR demonstrating alteration in luciferase activity in the Δ*pglL* compared to WT and Δ*pglL amrAB::S7-pglL-his₁₀* strains. Each data point corresponds to the mean of three independent biological replicates with a more detailed figure containing the plotted standard deviation provided in Supplementary Figure 4. B) Detailed analysis of three time points across the luciferase profiles are provided for the 12-hour (log), 16-hour (transition from log to stationary) and 20-hour (stationary) time points. For each time point the luciferase activity with strains grown with and without the presence of C8-HSL are shown. C) Z-scored heatmap of DNA bound proteins with significant alterations in abundance in Δ*pglL* or Δ*OGC* compared to WT reveal similar protein profiles for glycosylation-null strains compared to glycosylation-competent strains. D) DNA bound proteome analysis of CepR supports the reduction in the abundance of DNA bound CepR in Δ*pglL* and the partial restoration of CepR in Δ*pglL amrAB::S7-pglL-his₁₀.*

Figure 4. Biofilm formation and siderophore production are reduced in Δ*pglL*. A) 24-hour static biofilm assays demonstrate a decrease in biofilm formation in Δ*pglL* which is partially restored upon complementation. B and C) CAS assays demonstrates a reduction in zone of clearing in Δ*pglL* which is restored upon complementation.

Figure 5. The stability of the glycoprotein BCAL1086 and BCAL2974 are affected by loss of glycosylation. A) Proteomic analysis demonstrates BCAL1086 and BCAL2974 decrease

29

in abundance in the absence of glycosylation. B) Endogenous tagging of BCAL1086 confirms the loss of BCAL1086 in the Δ*pglL* background. C) Proteomics analysis of endogenous derived peptides demonstrates an increased abundance of BCAL1086-derived peptides in the absence of glycosylation. D) Analysis of endogenous peptides confirms the presence of unique peptide fragments from BCAL1086 in the Δ*pglL* background.

Figure 6. The loss of BCAL1086 or BCAL2974 does not affect phenotypes associated with ΔpglL. A) 24-hour static biofilm formation is unaffected in Δ*BCAL1086* and minimally affected in Δ*BCAL2974* compared to WT. B) CAS plate assays demonstrate similar zone of clearing in Δ*BCAL1086* and Δ*BCAL2974* compared to the K56-2 parent strain. C) Quantification of the zone of clearing demonstrates no significant alteration in siderophore activity in Δ*BCAL1086* and Δ*BCAL2974* compared to the K56-2 parent strain. D) Survival curve of *G. mellonella* infections. Data from three independent replicates of 8 to 10 larve for each biological group is shown with the standard deviation also denoted. Δ*BCAL1086* and Δ*BCAL2974* strains mirror the lethality of WT and Δ*pglL amrAB::native-pglL-his*$_{10}$.

Figure 7. Disruption of BCAL1086 and BCAL2974 does affect the proteome as Δ*pglL*. A) Pearson correlation analysis of K56-2 WT, Δ*BCAL2974*, Δ*BCAL1086*, Δ*pglL*, Δ*cepR*, Δ*cepI* and Δ*pglL amrAB::S7-pglL-his*$_{10}$ proteomes demonstrates K56-2 WT, Δ*BCAL2974*, Δ*BCAL1086* biological replicates cluster together while other strains form discrete clusters. B) Quantitative Proteome analysis of Δ*BCAL1086*, Δ*BCAL2974*, Δ*cepI*, Δ*cepR* and Δ*pglL* compared to wild type demonstrates minor proteome alterations compared to Δ*cepI*, Δ*cepR* and Δ*pglL*.

30

References

1. Vanlaere E, Baldwin A, Gevers D, Henry D, De Brandt E, LiPuma JJ, Mahenthiralingam E, Speert DP, Dowson C, Vandamme P. 2009. Taxon K, a complex within the Burkholderia cepacia complex, comprises at least two novel species, Burkholderia contaminans sp. nov. and Burkholderia lata sp. nov. Int J Syst Evol Microbiol 59:102-11.

2. De Smet B, Mayo M, Peeters C, Zlosnik JE, Spilker T, Hird TJ, LiPuma JJ, Kidd TJ, Kaestli M, Ginther JL, Wagner DM, Keim P, Bell SC, Jacobs JA, Currie BJ, Vandamme P. 2015. Burkholderia stagnalis sp. nov. and Burkholderia territorii sp. nov., two novel Burkholderia cepacia complex species from environmental and human sources. Int J Syst Evol Microbiol 65:2265-71.

3. Ong KS, Aw YK, Lee LH, Yule CM, Cheow YL, Lee SM. 2016. Burkholderia paludis sp. nov., an Antibiotic-Siderophore Producing Novel Burkholderia cepacia Complex Species, Isolated from Malaysian Tropical Peat Swamp Soil. Front Microbiol 7:2046.

4. Mahenthiralingam E, Urban TA, Goldberg JB. 2005. The multifarious, multireplicon Burkholderia cepacia complex. Nat Rev Microbiol 3:144-56.

5. Loutet SA, Valvano MA. 2010. A decade of Burkholderia cenocepacia virulence determinant research. Infect Immun 78:4088-100.

6. Huang CH, Jang TN, Liu CY, Fung CP, Yu KW, Wong WW. 2001. Characteristics of patients with Burkholderia cepacia bacteremia. J Microbiol Immunol Infect 34:215-9.

7. Hanulik V, Webber MA, Chroma M, Uvizl R, Holy O, Whitehead RN, Baugh S, Matouskova I, Kolar M. 2013. An outbreak of Burkholderia multivorans beyond cystic fibrosis patients. J Hosp Infect 84:248-51.

8. Liao CH, Chang HT, Lai CC, Huang YT, Hsu MS, Liu CY, Yang CJ, Hsueh PR. 2011. Clinical characteristics and outcomes of patients with Burkholderia cepacia bacteremia in an intensive care unit. Diagn Microbiol Infect Dis 70:260-6.

9. Regan KH, Bhatt J. 2019. Eradication therapy for Burkholderia cepacia complex in people with cystic fibrosis. Cochrane Database Syst Rev 4:CD009876.

10. Govan JR, Brown PH, Maddison J, Doherty CJ, Nelson JW, Dodd M, Greening AP, Webb AK. 1993. Evidence for transmission of Pseudomonas cepacia by social contact in cystic fibrosis. Lancet 342:15-9.

11. Fung SK, Dick H, Devlin H, Tullis E. 1998. Transmissibility and infection control implications of Burkholderia cepacia in cystic fibrosis. Can J Infect Dis 9:177-82.

12. Ledson MJ, Gallagher MJ, Jackson M, Hart CA, Walshaw MJ. 2002. Outcome of Burkholderia cepacia colonisation in an adult cystic fibrosis centre. Thorax 57:142-5.

13. Chaparro C, Maurer J, Gutierrez C, Krajden M, Chan C, Winton T, Keshavjee S, Scavuzzo M, Tullis E, Hutcheon M, Kesten S. 2001. Infection with Burkholderia cepacia in cystic fibrosis: outcome following lung transplantation. Am J Respir Crit Care Med 163:43-8.

14. Horsley A, Webb K, Bright-Thomas R, Govan J, Jones A. 2011. Can early Burkholderia cepacia complex infection in cystic fibrosis be eradicated with antibiotic therapy? Front Cell Infect Microbiol 1:18.

15. Kidd TJ, Douglas JM, Bergh HA, Coulter C, Bell SC. 2008. Burkholderia cepacia complex epidemiology in persons with cystic fibrosis from Australia and New Zealand. Res Microbiol 159:194-9.

16. Reik R, Spilker T, Lipuma JJ. 2005. Distribution of Burkholderia cepacia complex species among isolates recovered from persons with or without cystic fibrosis. J Clin Microbiol 43:2926-8.

17. Kenna DTD, Lilley D, Coward A, Martin K, Perry C, Pike R, Hill R, Turton JF. 2017. Prevalence of Burkholderia species, including members of Burkholderia cepacia complex, among UK cystic and non-cystic fibrosis patients. J Med Microbiol 66:490-501.

18. Lupo A, Isis E, Tinguely R, Endimiani A. 2015. Clonality and Antimicrobial Susceptibility of Burkholderia cepacia complex Isolates Collected from Cystic Fibrosis Patients during 1998-2013 in Bern, Switzerland. New Microbiol 38:281-8.

19. De Soyza A, McDowell A, Archer L, Dark JH, Elborn SJ, Mahenthiralingam E, Gould K, Corris PA. 2001. Burkholderia cepacia complex genomovars and pulmonary transplantation outcomes in patients with cystic fibrosis. Lancet 358:1780-1.

20. Gilchrist FJ, Webb AK, Bright-Thomas RJ, Jones AM. 2012. Successful treatment of cepacia syndrome with a combination of intravenous cyclosporin, antibiotics and oral corticosteroids. J Cyst Fibros 11:458-60.

21. Jassem AN, Zlosnik JE, Henry DA, Hancock RE, Ernst RK, Speert DP. 2011. In vitro susceptibility of Burkholderia vietnamiensis to aminoglycosides. Antimicrob Agents Chemother 55:2256-64.

22. Malott RJ, Steen-Kinnaird BR, Lee TD, Speert DP. 2012. Identification of hopanoid biosynthesis genes involved in polymyxin resistance in Burkholderia multivorans. Antimicrob Agents Chemother 56:464-71.

23. Hamad MA, Skeldon AM, Valvano MA. 2010. Construction of aminoglycoside-sensitive Burkholderia cenocepacia strains for use in studies of intracellular bacteria with the gentamicin protection assay. Appl Environ Microbiol 76:3170-6.

24. Coenye T. 2010. Social interactions in the Burkholderia cepacia complex: biofilms and quorum sensing. Future Microbiol 5:1087-99.

25. Van Acker H, Van Dijck P, Coenye T. 2014. Molecular mechanisms of antimicrobial tolerance and resistance in bacterial and fungal biofilms. Trends Microbiol 22:326-33.

26. Conway BA, Venu V, Speert DP. 2002. Biofilm formation and acyl homoserine lactone production in the Burkholderia cepacia complex. J Bacteriol 184:5678-85.

27. Savoia D, Zucca M. 2007. Clinical and environmental Burkholderia strains: biofilm production and intracellular survival. Curr Microbiol 54:440-4.

28. Schwab U, Leigh M, Ribeiro C, Yankaskas J, Burns K, Gilligan P, Sokol P, Boucher R. 2002. Patterns of epithelial cell invasion by different species of the Burkholderia cepacia complex in well-differentiated human airway epithelia. Infect Immun 70:4547-55.

29. Schwab U, Abdullah LH, Perlmutt OS, Albert D, Davis CW, Arnold RR, Yankaskas JR, Gilligan P, Neubauer H, Randell SH, Boucher RC. 2014. Localization of Burkholderia cepacia complex bacteria in cystic fibrosis lungs and interactions with Pseudomonas aeruginosa in hypoxic mucus. Infect Immun 82:4729-45.

30. Sajjan U, Corey M, Humar A, Tullis E, Cutz E, Ackerley C, Forstner J. 2001. Immunolocalisation of Burkholderia cepacia in the lungs of cystic fibrosis patients. J Med Microbiol 50:535-46.

31. Cunha MV, Sousa SA, Leitao JH, Moreira LM, Videira PA, Sa-Correia I. 2004. Studies on the involvement of the exopolysaccharide produced by cystic fibrosis-associated isolates of the Burkholderia cepacia complex in biofilm formation and in persistence of respiratory infections. J Clin Microbiol 42:3052-8.

32. Traverse CC, Mayo-Smith LM, Poltak SR, Cooper VS. 2013. Tangled bank of experimentally evolved Burkholderia biofilms reflects selection during chronic infections. Proc Natl Acad Sci U S A 110:E250-9.

33. Suppiger A, Schmid N, Aguilar C, Pessi G, Eberl L. 2013. Two quorum sensing systems control biofilm formation and virulence in members of the Burkholderia cepacia complex. Virulence 4:400-9.

34. Baldwin A, Sokol PA, Parkhill J, Mahenthiralingam E. 2004. The Burkholderia cepacia epidemic strain marker is part of a novel genomic island encoding both virulence and metabolism-associated genes in Burkholderia cenocepacia. Infect Immun 72:1537-47.

35. Malott RJ, O'Grady EP, Toller J, Inhulsen S, Eberl L, Sokol PA. 2009. A Burkholderia cenocepacia orphan LuxR homolog is involved in quorum-sensing regulation. J Bacteriol 191:2447-60.

36. Lutter E, Lewenza S, Dennis JJ, Visser MB, Sokol PA. 2001. Distribution of quorum-sensing genes in the Burkholderia cepacia complex. Infect Immun 69:4661-6.

37. Gotschlich A, Huber B, Geisenberger O, Togl A, Steidle A, Riedel K, Hill P, Tummler B, Vandamme P, Middleton B, Camara M, Williams P, Hardman A, Eberl L. 2001. Synthesis of multiple N-acylhomoserine lactones is wide-spread among the members of the Burkholderia cepacia complex. Syst Appl Microbiol 24:1-14.

38. Lewenza S, Conway B, Greenberg EP, Sokol PA. 1999. Quorum sensing in Burkholderia cepacia: identification of the LuxRI homologs CepRI. J Bacteriol 181:748-56.

39. Huber B, Riedel K, Hentzer M, Heydorn A, Gotschlich A, Givskov M, Molin S, Eberl L. 2001. The cep quorum-sensing system of Burkholderia cepacia H111 controls biofilm formation and swarming motility. Microbiology 147:2517-28.

40. Uehlinger S, Schwager S, Bernier SP, Riedel K, Nguyen DT, Sokol PA, Eberl L. 2009. Identification of specific and universal virulence factors in Burkholderia cenocepacia strains by using multiple infection hosts. Infect Immun 77:4102-10.

41. Chapalain A, Vial L, Laprade N, Dekimpe V, Perreault J, Deziel E. 2013. Identification of quorum sensing-controlled genes in Burkholderia ambifaria. Microbiologyopen 2:226-42.

42. Sokol PA, Sajjan U, Visser MB, Gingues S, Forstner J, Kooi C. 2003. The CepIR quorum-sensing system contributes to the virulence of Burkholderia cenocepacia respiratory infections. Microbiology 149:3649-58.

43. O'Grady EP, Viteri DF, Malott RJ, Sokol PA. 2009. Reciprocal regulation by the CepIR and CciIR quorum sensing systems in Burkholderia cenocepacia. BMC Genomics 10:441.

44. Subsin B, Chambers CE, Visser MB, Sokol PA. 2007. Identification of genes regulated by the cepIR quorum-sensing system in Burkholderia cenocepacia by high-throughput screening of a random promoter library. J Bacteriol 189:968-79.

45. Inhulsen S, Aguilar C, Schmid N, Suppiger A, Riedel K, Eberl L. 2012. Identification of functions linking quorum sensing with biofilm formation in Burkholderia cenocepacia H111. Microbiologyopen 1:225-42.

46. Kooi C, Corbett CR, Sokol PA. 2005. Functional analysis of the Burkholderia cenocepacia ZmpA metalloprotease. J Bacteriol 187:4421-9.

47. Kooi C, Subsin B, Chen R, Pohorelic B, Sokol PA. 2006. Burkholderia cenocepacia ZmpB is a broad-specificity zinc metalloprotease involved in virulence. Infect Immun 74:4083-93.

48. Lewenza S, Sokol PA. 2001. Regulation of ornibactin biosynthesis and N-acyl-L-homoserine lactone production by CepR in Burkholderia cepacia. J Bacteriol 183:2212-8.

49. Nothaft H, Szymanski CM. 2013. Bacterial protein N-glycosylation: new perspectives and applications. J Biol Chem 288:6912-20.

50. Szymanski CM, Wren BW. 2005. Protein glycosylation in bacterial mucosal pathogens. Nat Rev Microbiol 3:225-37.

51. Koomey M. 2019. O-linked protein glycosylation in bacteria: snapshots and current perspectives. Curr Opin Struct Biol 56:198-203.

52. Fletcher CM, Coyne MJ, Villa OF, Chatzidaki-Livanis M, Comstock LE. 2009. A general O-glycosylation system important to the physiology of a major human intestinal symbiont. Cell 137:321-31.

53. Elhenawy W, Scott NE, Tondo ML, Orellano EG, Foster LJ, Feldman MF. 2016. Protein O-linked glycosylation in the plant pathogen Ralstonia solanacearum. Glycobiology 26:301-11.

54. Harding CM, Nasr MA, Kinsella RL, Scott NE, Foster LJ, Weber BS, Fiester SE, Actis LA, Tracy EN, Munson RS, Jr., Feldman MF. 2015. Acinetobacter strains carry two functional oligosaccharyltransferases, one devoted exclusively to type IV pilin, and the other one dedicated to O-glycosylation of multiple proteins. Mol Microbiol 96:1023-41.

55. Iwashkiw JA, Seper A, Weber BS, Scott NE, Vinogradov E, Stratilo C, Reiz B, Cordwell SJ, Whittal R, Schild S, Feldman MF. 2012. Identification of a general O-linked protein glycosylation system in Acinetobacter baumannii and its role in virulence and biofilm formation. PLoS Pathog 8:e1002758.

56. Lithgow KV, Scott NE, Iwashkiw JA, Thomson EL, Foster LJ, Feldman MF, Dennis JJ. 2014. A general protein O-glycosylation system within the Burkholderia cepacia complex is involved in motility and virulence. Mol Microbiol 92:116-37.

57. Nothaft H, Scott NE, Vinogradov E, Liu X, Hu R, Beadle B, Fodor C, Miller WG, Li J, Cordwell SJ, Szymanski CM. 2012. Diversity in the protein N-glycosylation pathways within the Campylobacter genus. Mol Cell Proteomics 11:1203-19.

58. Scott NE, Kinsella RL, Edwards AV, Larsen MR, Dutta S, Saba J, Foster LJ, Feldman MF. 2014. Diversity within the O-linked protein glycosylation systems of acinetobacter species. Mol Cell Proteomics 13:2354-70.

59. Coyne MJ, Fletcher CM, Chatzidaki-Livanis M, Posch G, Schaffer C, Comstock LE. 2013. Phylum-wide general protein O-glycosylation system of the Bacteroidetes. Mol Microbiol 88:772-83.

60. Posch G, Pabst M, Neumann L, Coyne MJ, Altmann F, Messner P, Comstock LE, Schaffer C. 2012. "Cross-glycosylation" of proteins in Bacteriodales species. Glycobiology doi:10.1093/glycob/cws172.

61. Iwashkiw JA, Vozza NF, Kinsella RL, Feldman MF. 2013. Pour some sugar on it: the expanding world of bacterial protein O-linked glycosylation. Mol Microbiol 89:14-28.

62. Nothaft H, Szymanski CM. 2010. Protein glycosylation in bacteria: sweeter than ever. Nat Rev Microbiol 8:765-78.

63. Cain JA, Dale AL, Niewold P, Klare WP, Man L, White MY, Scott NE, Cordwell SJ. 2019. Proteomics reveals multiple phenotypes associated with N-linked glycosylation in Campylobacter jejuni. Mol Cell Proteomics doi:10.1074/mcp.RA118.001199.

64. Abouelhadid S, North SJ, Hitchen P, Vohra P, Chintoan-Uta C, Stevens M, Dell A, Cuccui J, Wren BW. 2019. Quantitative Analyses Reveal Novel Roles for N-Glycosylation in a Major Enteric Bacterial Pathogen. MBio 10.

65. Fathy Mohamed Y, Scott NE, Molinaro A, Creuzenet C, Ortega X, Lertmemongkolchai G, Tunney MM, Green H, Jones AM, DeShazer D, Currie BJ, Foster LJ, Ingram R, De Castro C, Valvano MA. 2019. A general protein O-glycosylation machinery conserved in Burkholderia species improves bacterial fitness and elicits glycan immunogenicity in humans. J Biol Chem doi:10.1074/jbc.RA119.009671.

66.   Sambrook J, E. F. Fritsch, and T. Maniatis. 1990. Molecular cloning: a laboratory manual. Cold Spring Harbor Laboratory, Cold Spring Harbor, N.Y.

67.   Gibson DG, Young L, Chuang RY, Venter JC, Hutchison CA, 3rd, Smith HO. 2009. Enzymatic assembly of DNA molecules up to several hundred kilobases. Nat Methods 6:343-5.

68.   Flannagan RS, Linn T, Valvano MA. 2008. A system for the construction of targeted unmarked gene deletions in the genus Burkholderia. Environ Microbiol 10:1652-60.

69.   Aubert DF, Hamad MA, Valvano MA. 2014. A markerless deletion method for genetic manipulation of Burkholderia cenocepacia and other multidrug-resistant gram-negative bacteria. Methods Mol Biol 1197:311-27.

70.   Qin H, Wang Y. 2009. Exploring DNA-binding proteins with in vivo chemical cross-linking and mass spectrometry. J Proteome Res 8:1983-91.

71.   Dejardin J, Kingston RE. 2009. Purification of proteins associated with specific genomic Loci. Cell 136:175-86.

72.   Humphrey SJ, Azimifar SB, Mann M. 2015. High-throughput phosphoproteomics reveals in vivo insulin signaling dynamics. Nat Biotechnol 33:990-5.

73.   Parker BL, Burchfield JG, Clayton D, Geddes TA, Payne RJ, Kiens B, Wojtaszewski JFP, Richter EA, James DE. 2017. Multiplexed Temporal Quantification of the Exercise-regulated Plasma Peptidome. Mol Cell Proteomics 16:2055-2068.

74.   Scott NE, Parker BL, Connolly AM, Paulech J, Edwards AV, Crossett B, Falconer L, Kolarich D, Djordjevic SP, Hojrup P, Packer NH, Larsen MR, Cordwell SJ. 2011. Simultaneous Glycan-Peptide Characterization Using Hydrophilic Interaction Chromatography and Parallel Fragmentation by CID, Higher Energy Collisional Dissociation, and Electron Transfer Dissociation MS Applied to the N-Linked Glycoproteome of Campylobacter jejuni. Mol Cell Proteomics 10:M000031MCP201.

75.   Ishihama Y, Rappsilber J, Mann M. 2006. Modular stop and go extraction tips with stacked disks for parallel and multidimensional Peptide fractionation in proteomics. J Proteome Res 5:988-94.

76.   Rappsilber J, Mann M, Ishihama Y. 2007. Protocol for micro-purification, enrichment, pre-fractionation and storage of peptides for proteomics using StageTips. Nat Protoc 2:1896-906.

77.   Peterson AC, Russell JD, Bailey DJ, Westphall MS, Coon JJ. 2012. Parallel reaction monitoring for high resolution and high mass accuracy quantitative, targeted proteomics. Mol Cell Proteomics 11:1475-88.

78.   Cox J, Mann M. 2008. MaxQuant enables high peptide identification rates, individualized p.p.b.-range mass accuracies and proteome-wide protein quantification. Nat Biotechnol 26:1367-72.

79.   Varga JJ, Losada L, Zelazny AM, Kim M, McCorrison J, Brinkac L, Sampaio EP, Greenberg DE, Singh I, Heiner C, Ashby M, Nierman WC, Holland SM, Goldberg JB. 2013. Draft Genome Sequences of Burkholderia cenocepacia ET12 Lineage Strains K56-2 and BC7. Genome Announc 1.

80.   Cox J, Hein MY, Luber CA, Paron I, Nagaraj N, Mann M. 2014. Accurate proteome-wide label-free quantification by delayed normalization and maximal peptide ratio extraction, termed MaxLFQ. Mol Cell Proteomics 13:2513-26.

81.   Tyanova S, Temu T, Sinitcyn P, Carlson A, Hein MY, Geiger T, Mann M, Cox J. 2016. The Perseus computational platform for comprehensive analysis of (prote)omics data. Nat Methods 13:731-40.

82.   Winsor GL, Khaira B, Van Rossum T, Lo R, Whiteside MD, Brinkman FS. 2008. The Burkholderia Genome Database: facilitating flexible queries and comparative analyses. Bioinformatics 24:2803-4.

83.   Holden MT, Seth-Smith HM, Crossman LC, Sebaihia M, Bentley SD, Cerdeno-Tarraga AM, Thomson NR, Bason N, Quail MA, Sharp S, Cherevach I, Churcher C, Goodhead I, Hauser H, Holroyd N, Mungall K, Scott P, Walker D, White B, Rose H, Iversen P, Mil-Homens D, Rocha EP, Fialho AM, Baldwin A, Dowson C, Barrell BG, Govan JR, Vandamme P, Hart CA, Mahenthiralingam E, Parkhill J. 2009. The genome of Burkholderia cenocepacia J2315, an epidemic pathogen of cystic fibrosis patients. J Bacteriol 191:261-77.

84.   Vizcaino JA, Csordas A, del-Toro N, Dianes JA, Griss J, Lavidas I, Mayer G, Perez-Riverol Y, Reisinger F, Ternent T, Xu QW, Wang R, Hermjakob H. 2016. 2016 update of the PRIDE database and its related tools. Nucleic Acids Res 44:D447-56.

85.   Malott RJ, Baldwin A, Mahenthiralingam E, Sokol PA. 2005. Characterization of the cciIR quorum-sensing system in Burkholderia cenocepacia. Infect Immun 73:4982-92.

86.   Aubert DF, O'Grady EP, Hamad MA, Sokol PA, Valvano MA. 2013. The Burkholderia cenocepacia sensor kinase hybrid AtsR is a global regulator modulating quorum-sensing signalling. Environ Microbiol 15:372-85.

87.   Duan K, Dammel C, Stein J, Rabin H, Surette MG. 2003. Modulation of Pseudomonas aeruginosa gene expression by host microflora through interspecies communication. Mol Microbiol 50:1477-91.

88.   Le Guillouzer S, Groleau MC, Deziel E. 2017. The Complex Quorum Sensing Circuitry of Burkholderia thailandensis Is Both Hierarchically and Homeostatically Organized. MBio 8.

89.   Peeters E, Nelis HJ, Coenye T. 2008. Resistance of planktonic and biofilm-grown Burkholderia cepacia complex isolates to the transition metal gallium. J Antimicrob Chemother 61:1062-5.

90.   Tomlin KL, Malott RJ, Ramage G, Storey DG, Sokol PA, Ceri H. 2005. Quorum-sensing mutations affect attachment and stability of Burkholderia cenocepacia biofilms. Appl Environ Microbiol 71:5208-18.

91.   O'Toole GA. 2011. Microtiter dish biofilm formation assay. J Vis Exp doi:10.3791/2437.

92.   Seed KD, Dennis JJ. 2008. Development of Galleria mellonella as an alternative infection model for the Burkholderia cepacia complex. Infect Immun 76:1267-75.

93.   Schwyn B, Neilands JB. 1987. Universal chemical assay for the detection and determination of siderophores. Anal Biochem 160:47-56.

94.   Louden BC, Haarmann D, Lynne AM. 2011. Use of Blue Agar CAS Assay for Siderophore Detection. J Microbiol Biol Educ 12:51-3.

95.   Edgington-Mitchell LE, Barlow N, Aurelio L, Samha A, Szabo M, Graham B, Bunnett N. 2017. Fluorescent diphenylphosphonate-based probes for detection of serine protease activity during inflammation. Bioorg Med Chem Lett 27:254-260.

96.   Kasperkiewicz P, Altman Y, D'Angelo M, Salvesen GS, Drag M. 2017. Toolbox of Fluorescent Probes for Parallel Imaging Reveals Uneven Location of Serine Proteases in Neutrophils. J Am Chem Soc 139:10115-10125.

97.   Kasperkiewicz P, Poreba M, Snipas SJ, Parker H, Winterbourn CC, Salvesen GS, Drag M. 2014. Design of ultrasensitive probes for human neutrophil elastase through hybrid combinatorial substrate library profiling. Proc Natl Acad Sci U S A 111:2518-23.

98.   Liu Y, Patricelli MP, Cravatt BF. 1999. Activity-based protein profiling: the serine hydrolases. Proc Natl Acad Sci U S A 96:14694-9.

99.   Gebhart C, Ielmini MV, Reiz B, Price NL, Aas FE, Koomey M, Feldman MF. 2012. Characterization of exogenous bacterial oligosaccharyltransferases in Escherichia coli

reveals the potential for O-linked protein glycosylation in Vibrio cholerae and Burkholderia thailandensis. Glycobiology 22:962-74.

100. Chambers CE, Lutter EI, Visser MB, Law PP, Sokol PA. 2006. Identification of potential CepR regulated genes using a cep box motif-based search of the Burkholderia cenocepacia genome. BMC Microbiol 6:104.

101. Huber B, Feldmann F, Kothe M, Vandamme P, Wopperer J, Riedel K, Eberl L. 2004. Identification of a novel virulence factor in Burkholderia cenocepacia H111 required for efficient slow killing of Caenorhabditis elegans. Infect Immun 72:7220-30.

102. O'Grady EP, Nguyen DT, Weisskopf L, Eberl L, Sokol PA. 2011. The Burkholderia cenocepacia LysR-type transcriptional regulator ShvR influences expression of quorum-sensing, protease, type II secretion, and afc genes. J Bacteriol 193:163-76.

103. Schmid N, Pessi G, Deng Y, Aguilar C, Carlier AL, Grunau A, Omasits U, Zhang LH, Ahrens CH, Eberl L. 2012. The AHL- and BDSF-dependent quorum sensing systems control specific and overlapping sets of genes in Burkholderia cenocepacia H111. PLoS One 7:e49966.

104. O'Grady EP, Viteri DF, Sokol PA. 2012. A unique regulator contributes to quorum sensing and virulence in Burkholderia cenocepacia. PLoS One 7:e37611.

105. Hoffman EA, Frey BL, Smith LM, Auble DT. 2015. Formaldehyde crosslinking: a tool for the study of chromatin complexes. J Biol Chem 290:26404-11.

106. Larsen JC, Szymanski C, Guerry P. 2004. N-linked protein glycosylation is required for full competence in Campylobacter jejuni 81-176. J Bacteriol 186:6508-14.

107. Nothaft H, Szymanski CM. 2019. New discoveries in bacterial N-glycosylation to expand the synthetic biology toolbox. Curr Opin Chem Biol 53:16-24.

108. Young NM, Brisson JR, Kelly J, Watson DC, Tessier L, Lanthier PH, Jarrell HC, Cadotte N, St Michael F, Aberg E, Szymanski CM. 2002. Structure of the N-linked glycan present on multiple glycoproteins in the Gram-negative bacterium, Campylobacter jejuni. J Biol Chem 277:42530-9.

109. Wacker M, Linton D, Hitchen PG, Nita-Lazar M, Haslam SM, North SJ, Panico M, Morris HR, Dell A, Wren BW, Aebi M. 2002. N-linked glycosylation in Campylobacter jejuni and its functional transfer into E. coli. Science 298:1790-3.

110. Wong YC, Abd El Ghany M, Ghazzali RNM, Yap SJ, Hoh CC, Pain A, Nathan S. 2018. Genetic Determinants Associated With in Vivo Survival of Burkholderia cenocepacia in the Caenorhabditis elegans Model. Front Microbiol 9:1118.
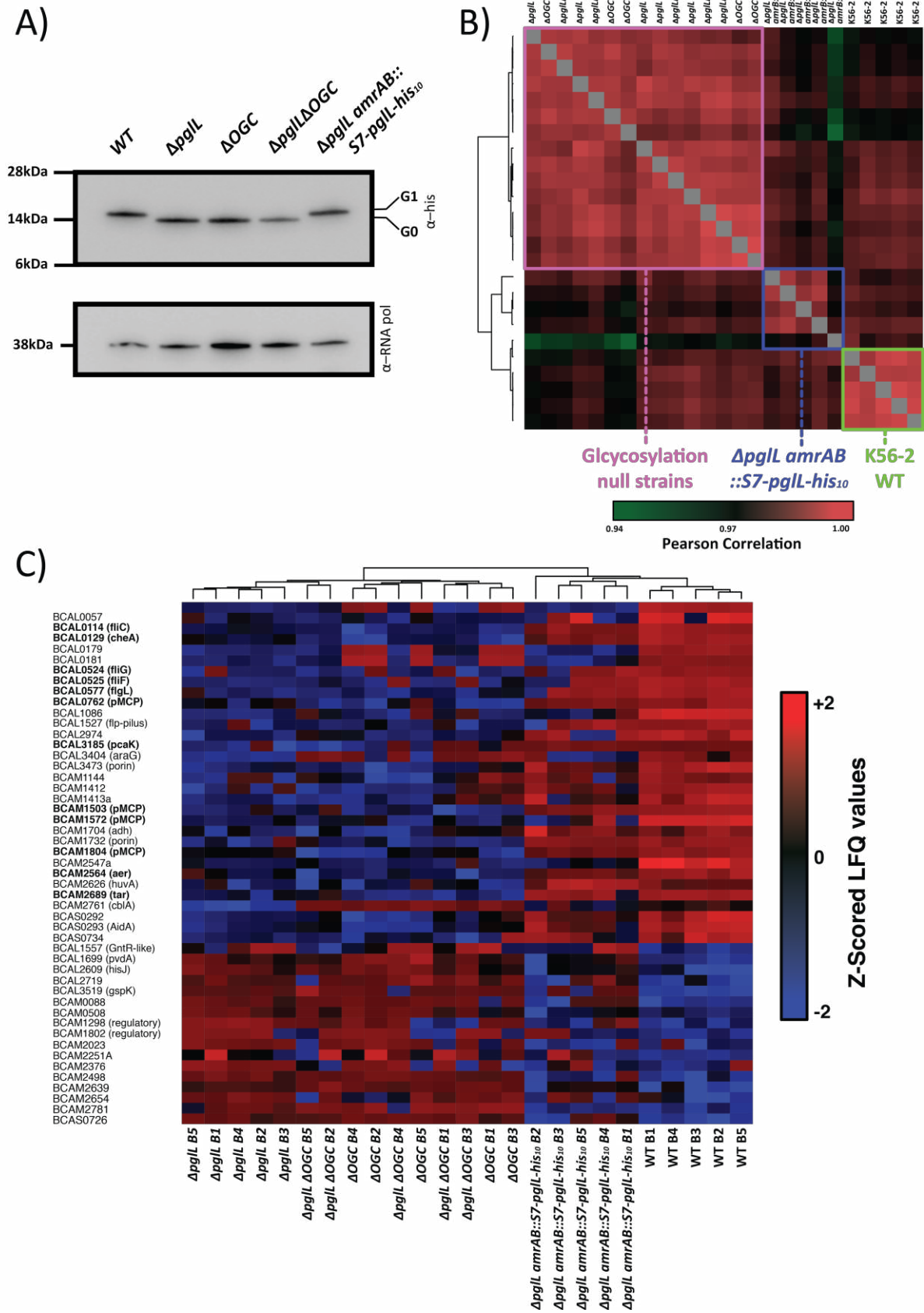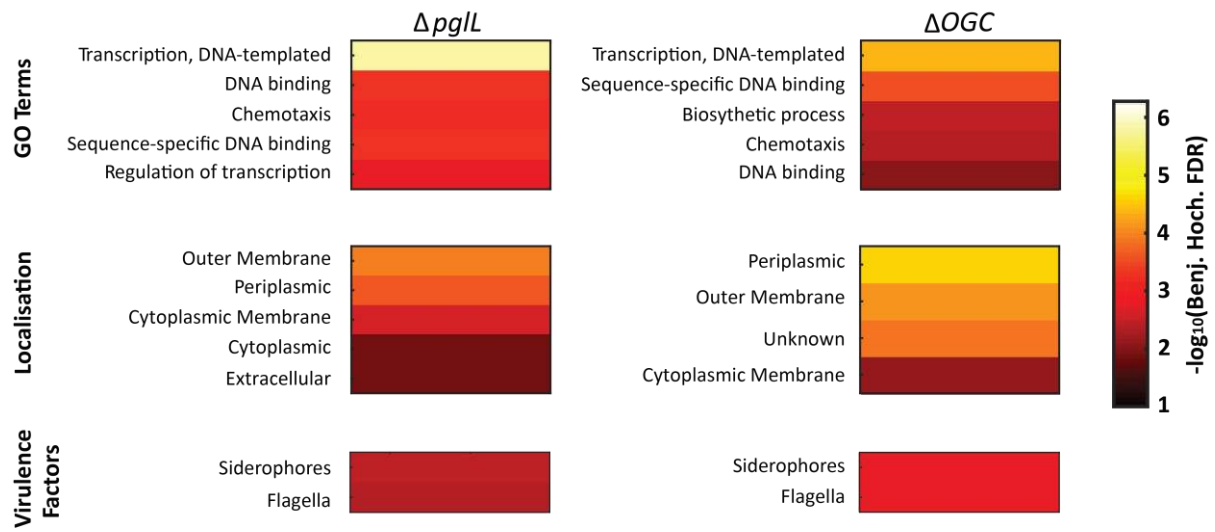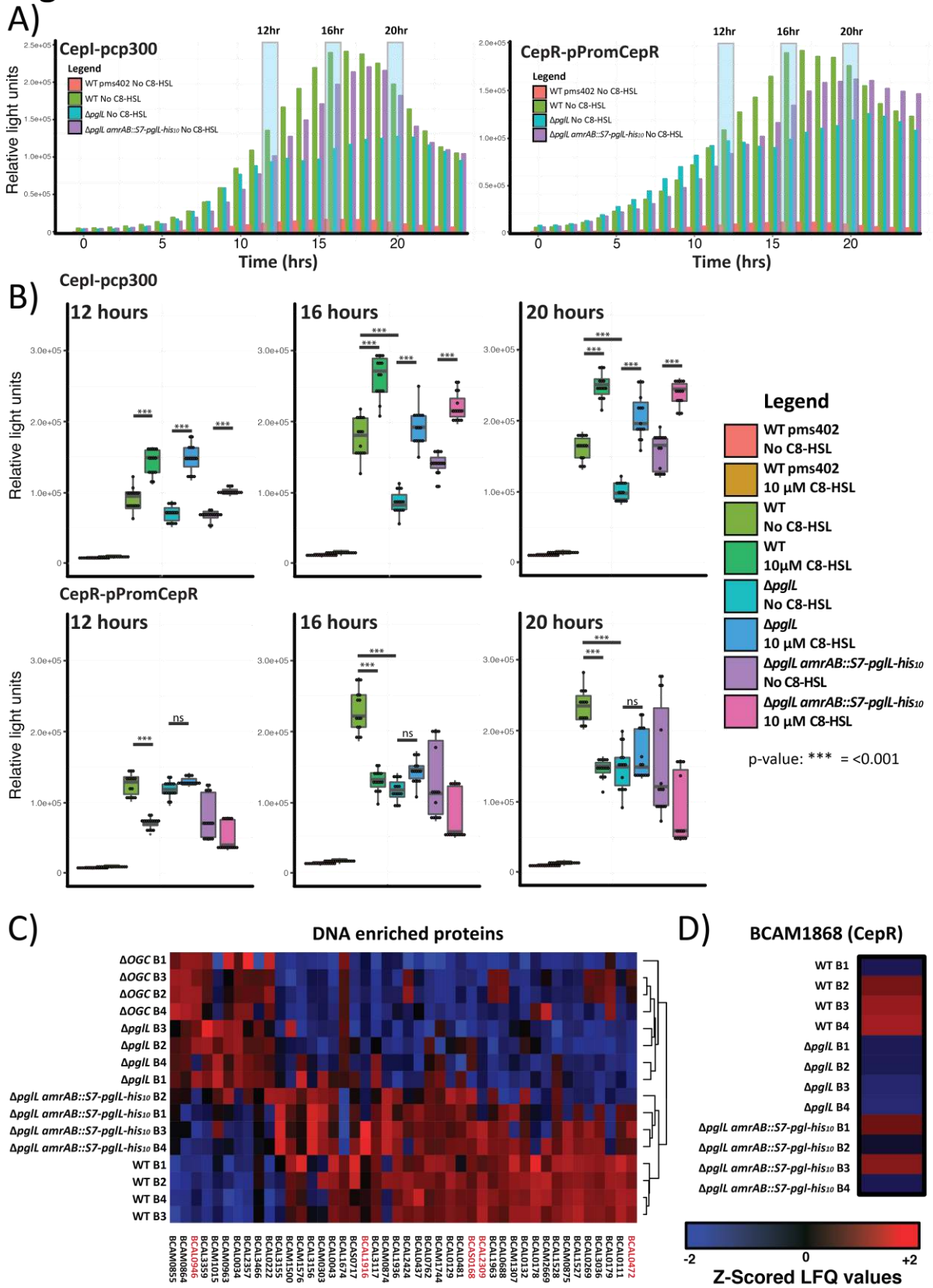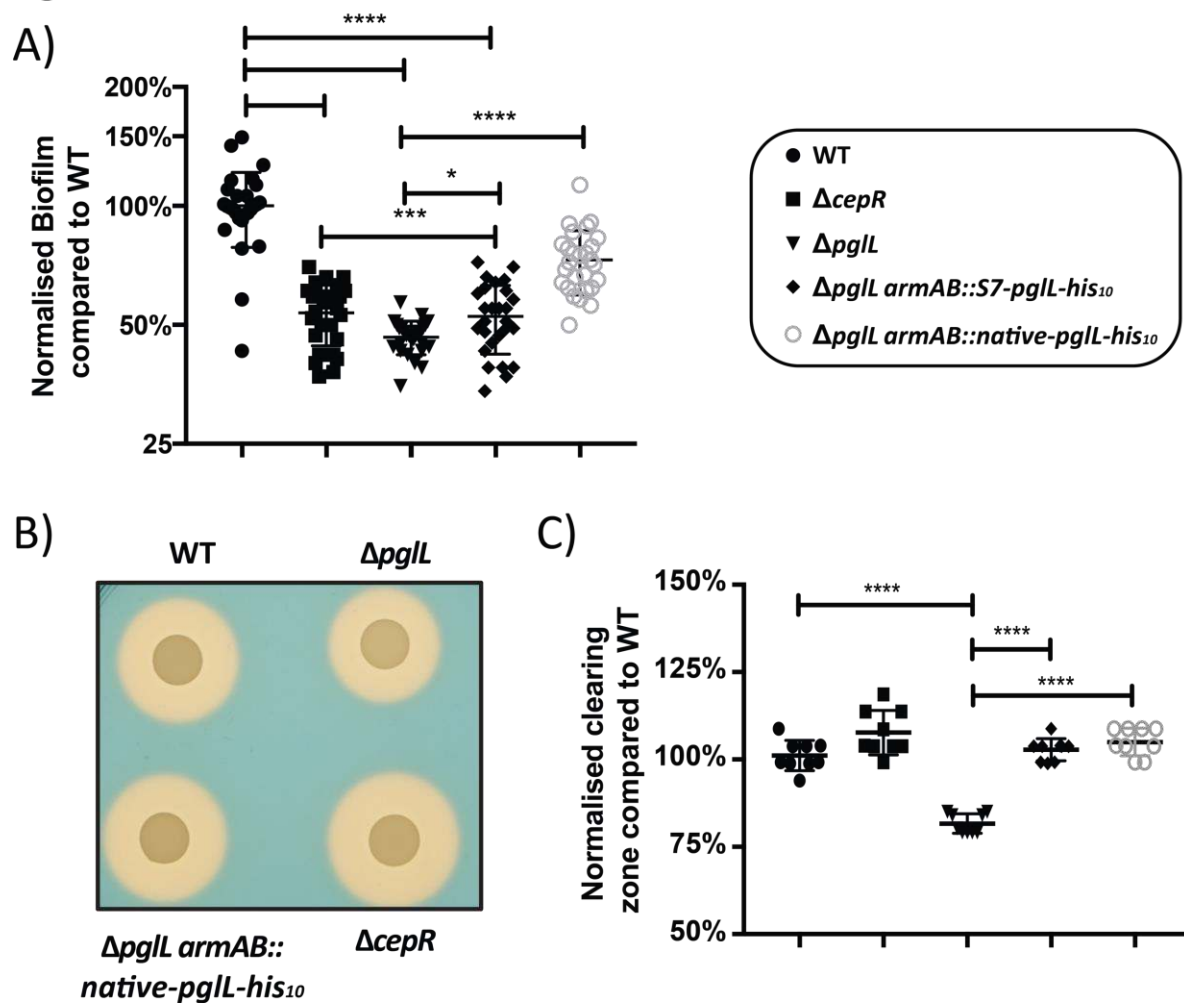
Figure 1

Figure 2

Figure 3

Figure 4

A)

Legend:
- ● WT
- ■ ΔcepR
- ▼ ΔpglL
- ◆ ΔpglL armAB::S7-pglL-his$_{10}$
- ○ ΔpglL armAB::native-pglL-his$_{10}$

B)

WT   ΔpglL

ΔpglL armAB::   ΔcepR
native-pglL-his$_{10}$

C)

Figure 5

Figure 6

Figure 7